

# Preparation and Characterization of Nickel–Polystyrene Nanocomposite by Ultrasound Irradiation

R. Vijaya Kumar, Yu. Koltypin, O. Palchik, A. Gedanken

Department of Chemistry, Bar-Ilan University, Ramat-Gan 52900, Israel

Received 13 April 2001; accepted 14 January 2002

**ABSTRACT:** Well-dispersed nickel nanoparticles in polystyrene were obtained by a sonochemical method. The properties of the as-prepared nanocomposite materials were characterized by XRD, TEM, EDAX, TGA, DSC, and a vibrating sample magnetometer (VSM). The nickel particles were 5 nm in diameter and were very well dispersed in the polystyrene. The magnetization measurements established that the as-prepared nanocomposite materials are superparamagnetic due to their small size. The saturation magne-

tization (30.1 emu/g) and coercivity (5 Oe) of the materials were significantly smaller than were those of the bulk nickel, reflecting the nanoparticle nature. © 2002 Wiley Periodicals, Inc. *J Appl Polym Sci* 86: 160–165, 2002

**Key words:** sonochemistry; nickel–polymer composite; magnetic materials; nanocomposites

## INTRODUCTION

Due to their extremely small size and large specific surface area, nanoparticles usually exhibit unusual physical and chemical properties compared to that of bulk materials.<sup>1,2</sup> The use of a polymer matrix as an environment for *in situ* nanoparticle growth combines, synergistically, the properties of both the host polymer matrix and the discrete nanoparticles formed within it. The nanoparticles of metals and metal oxides embedded in polymer matrices have attracted increasing interest because of the unique properties displayed by materials containing such nanoparticles. Such composite materials are expected to have novel magnetic, optical, electrical, catalytic, and mechanical properties.<sup>3–7</sup> Many techniques have been exploited to prepare metal- or metal oxide-polymer composites.<sup>8–14</sup> Copper-polymer composite materials were prepared by Huang et al.<sup>15</sup> and Lyons et al.<sup>16</sup> by two different methods: by *in situ* reduction within a Cu<sup>+</sup>-poly(itaconic acid-co-acrylic acid) complex and by thermal decomposition of a copper formate-poly(2-vinylpyridine) complex, respectively. Recently, Sidorov et al.<sup>17</sup> prepared cobalt nanoparticles embedded in hypercrosslinked polystyrene by a thermolysis technique. Recently, Zach and Penner<sup>18</sup> and Chen and Wu<sup>19</sup> prepared pristine nickel nanoparticles by two different methods: electrochemical and by microemulsions, respectively. Chaudret and coworkers<sup>20</sup> synthesized nickel

nanoparticles in polyvinylpyrrolidone by reduction of Ni(COD)<sub>2</sub> by H<sub>2</sub> in polyvinylpyrrolidone. Recently, Wang and Pan<sup>21</sup> prepared a poly(sty-co-MMA)-Ni composite by a chemical metal deposition method.

Sonochemical processing has proven to be a useful technique for generating novel materials with unusual properties. Sonochemistry arises from the acoustic cavitation phenomenon, that is, the formation, growth, and implosive collapse of bubbles in a liquid medium.<sup>22</sup> The extremely high temperatures (>5000 K), pressures (>20 MPa), and very high cooling rates (>10<sup>7</sup> K s<sup>-1</sup>)<sup>23</sup> attained during cavity collapse lead to many unique properties of the irradiated solution. Using these extreme conditions, Suslick et al. prepared amorphous iron<sup>23</sup> by sonochemical decomposition of metal carbonyls dissolved in an alkane. We successfully prepared amorphous nickel,<sup>24</sup> coating of nanosized nickel on alumina<sup>25</sup> and silica<sup>26</sup> microspheres, and encapsulation of nickel nanoparticles in carbon<sup>27</sup> and various magnetic polymer composite materials.<sup>28</sup> However, all these methods used, as a starting material, Ni(CO)<sub>4</sub>, which is a hazardous material no longer commercially available.

In the present investigation, we report on the preparation of a nickel-polystyrene nanocomposite using a sonochemical method. The precursor for the current study was nickel formate.

## EXPERIMENTAL

### Preparation of nickel formate precursor [Ni(HCO<sub>2</sub>)<sub>2</sub> · 2H<sub>2</sub>O]

Nickel formate was prepared according to a previously described method.<sup>29</sup> A typical procedure for the

Correspondence to: A. Gedanken (gedanken@mail.biu.ac.il).

Contract grant sponsors: Israeli Ministry of Science, Culture and Sports; German Ministry of Science; INTAS.

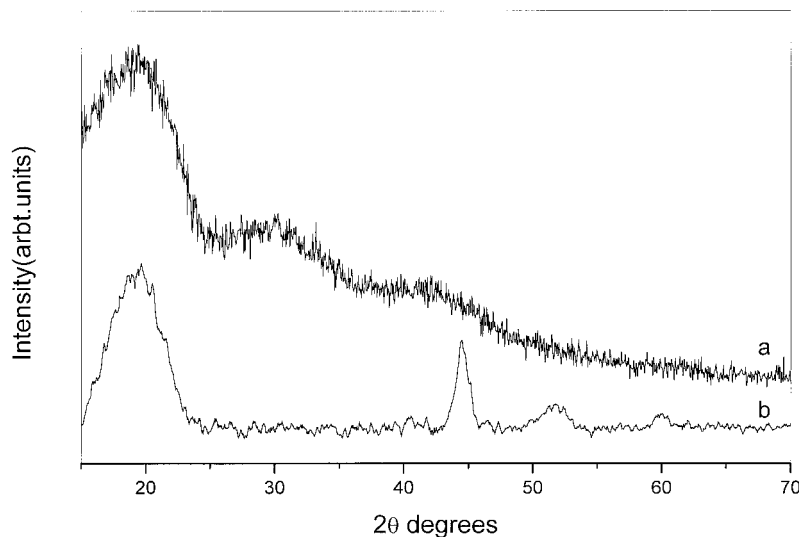


**Figure 1** X-ray diffractions pattern of (a) pristine polystyrene and (b) as-prepared nanocomposite material.

preparation of nickel formate is as follows: Two grams of crystalline  $\text{Ni}(\text{CH}_3\text{CO}_2)_2 \cdot 4\text{H}_2\text{O}$  and 8 mL of water are poured into a 100-mL conical flask. The mixture is heated while stirring in a water bath at  $\sim 60\text{--}80^\circ\text{C}$  until a clear green solution results (less than 5 min is required). Then, 4 mL of formic acid is added to the warm solution, the conical flask is cooled in an ice bath, and 12 mL of ethanol is added with stirring. The light green microcrystalline precipitate is filtered, washed with ethanol and diethyl ether several times, and dried in a vacuum overnight.

The product was analyzed using a C, H, N analyzer and EDAX methods:

ANAL. Calcd: Ni, 31.8%; C, 13.0%; and H, 2.2%. Found: Ni, 31.5%; C, 12.94%; H, 2.45%.

The FTIR spectra of nickel formate shows characteristic peaks at  $\sim 778, 802, 850, 889, 1070, 1362, 1383, 1580\text{ cm}^{-1}$  ( $\nu_{\text{HCOO}^-}$ ),  $1401\text{ cm}^{-1}$  ( $\nu_{\text{CO}}$ ), and  $2869, 2890,$  and  $2990\text{ cm}^{-1}$  ( $\nu_{\text{CH}}$ ).

The preparation of the nickel-polystyrene composite was carried out by the sonochemical method. Typically, 500 mg of nickel formate and 1 g of polystyrene (Aldrich;  $M_w = 350,000$ ) are dissolved in 100 mL of *N,N*-dimethylformamide (DMF) and irradiated with a high-intensity ultrasonic horn (Ti-horn, 20 kHz; Sonics Int. Materials Inc., CT) under 1.5 atm of Ar/H<sub>2</sub> at room temperature for 3 h. The product is washed thoroughly with methanol in an inert glove box ( $\text{O}_2 < 2\text{ ppm}$ ) and dried in a vacuum overnight. The XRD measurements were carried out with a Bruker X-ray diffractometer D8. EDAX measurements were carried out on a JEOL-JSM 840 scanning electron microscope. Elemental analysis was carried out by an Eager 200 C, H, N analyzer. Magnetization was measured using a vibrating sample magnetometer (VSM-Oxford 3001). DSC measurements were carried out on a Mettler DSC 30 using argon as the carrying gas. Thermogravimetric

analysis (TGA) was carried out using a Mettler-TGA/STDA 851.

## RESULTS AND DISCUSSION

A nickel-polystyrene nanocomposite was obtained by sonication of nickel formate in a DMF solution with polystyrene under an Ar/H<sub>2</sub> atmosphere. Figure 1 displays the XRD patterns of (a) pristine polystyrene and (b) the as-prepared nickel-polystyrene nanocomposite. Figure 1(b) indicates that the as-prepared composite material is crystalline. The XRD diffraction patterns match those of metallic nickel (JCPDS card no: 04-0850). The diffraction line around  $2\theta = 20^\circ$  corresponds to the polystyrene. The particles sizes, calculated using the Debye-Scherrer formula,<sup>30</sup> are 8 nm for the as-prepared composite material. C, H, N and EDAX analyses revealed that the as-prepared nickel-polystyrene composite contains 7.5% of nickel nanoparticles and 92.5% of polystyrene. Figure 2 illustrates a TEM image of the as-prepared composite material. It clearly shows the excellent dispersion of metallic nickel nanoparticles over the entire polymer volume. The particle sizes measured from the TEM picture are about 5 nm.

Figure 3 shows DSC curves of (a) pristine polystyrene and (b) the as-prepared composite material. The broad endothermic peak detected in Figure 3(a) at about  $106^\circ\text{C}$  is attributed to the glass transition temperature; the second endothermic peak at about  $410^\circ\text{C}$  is attributed to the structural decomposition of the polystyrene. In Figure 3(b), the broad endothermic peak about  $83^\circ\text{C}$  is attributed to the glass transition temperature of the composite; the sharp exothermic peak at about  $458^\circ\text{C}$  is attributed to the crosslinking of polystyrene<sup>31</sup> in the presence of nickel nanoparticles. The reason for the lowering of the glass transition

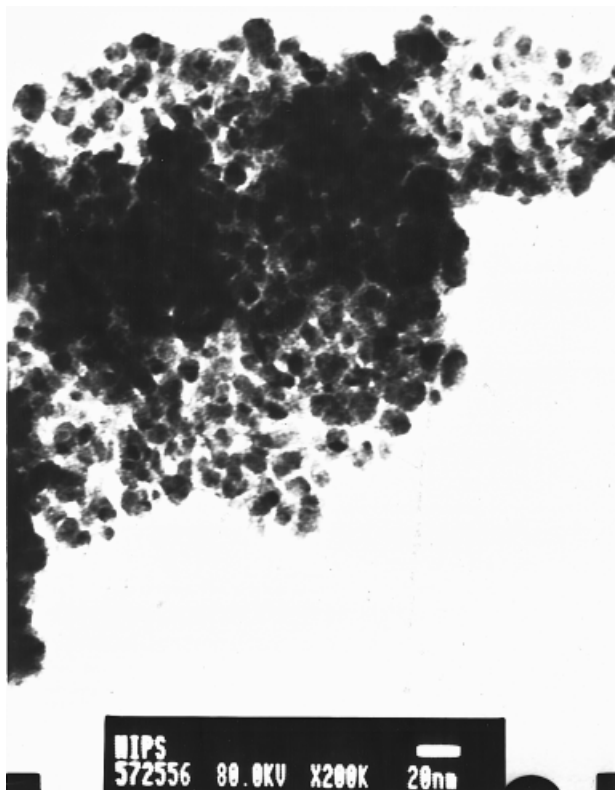


**Figure 2** Transmission electron micrographs of as-prepared nanocomposite material.

temperature could be the existence of nickel nanoparticles as an impurity in the as-prepared composite material. We did not observe an endothermic peak due to the structural decomposition of polystyrene. The reason for this could be that decomposition and crosslinking take place at almost the same temperature range, and the resulting exothermic peak is stron-

ger than is the endothermic peak and overshadows it. We also did not observe the decomposition of crosslinked polystyrene, which takes place at higher temperatures.<sup>32</sup> This is because of experimental limitations.

We carried out TGA measurements to obtain information on the stability of the polymer and the effect of the nickel nanoparticles on its stability. Figure 4 shows the TGA curve of (a) pristine polystyrene and (b) the as-prepared composite material. Pristine polystyrene disintegrates at  $\sim 410^\circ\text{C}$ , while the as-prepared composite material is stable to  $\sim 445^\circ\text{C}$  and continues to lose weight to  $585^\circ\text{C}$ . This weight loss is due to the decomposition of crosslinked polystyrene<sup>32</sup> in accord with the corresponding DSC results. The percentage of the total weight loss of polystyrene obtained from the TGA results matches that of the C, H, N and EDAX results. The reason for an increase in the decomposition temperature of the as-prepared composite material could be the polystyrene crosslinking in the presence of nickel nanoparticles. This behavior was observed in the DSC as well.

Nickel is known to be one of the important magnetic materials. The magnetic properties of the as-prepared composite material were analyzed by a vibrating sample magnetometer (VSM). Figure 5 shows the room-temperature magnetization loop of the as-prepared composite material, exhibiting a saturation magnetization of  $30.1 \text{ emu/g}$  nickel and a coercive field of  $5 \text{ Oe}$ . For comparison, we note that the saturation magnetization and the coercive field for commercial metallic nickel powder at  $300 \text{ K}$  are about  $55 \text{ emu/g}$  and  $100 \text{ Oe}$ , respectively.<sup>3</sup> Since the nickel nanoparticles in the polystyrene matrix are smaller than are those of commercial metallic nickel powder, the magnetization

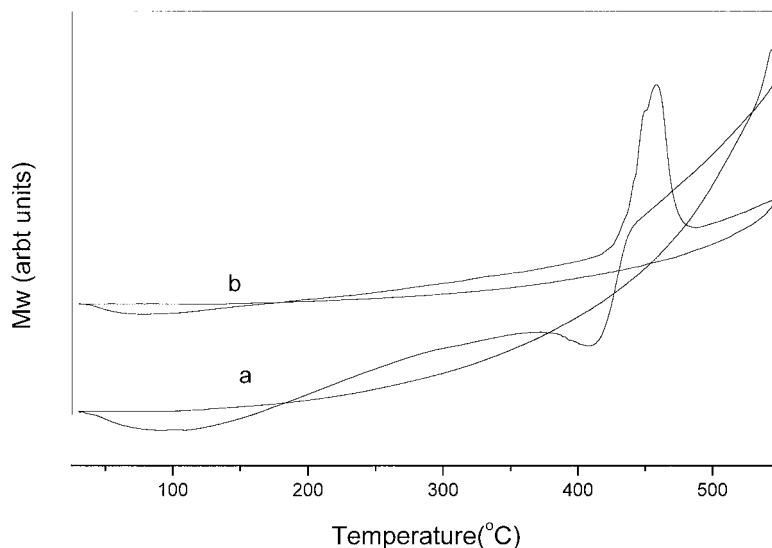


**Figure 3** DSC curves of (a) pristine polystyrene and (b) as-prepared nanocomposite material. The heating rate was  $10^\circ\text{C min}^{-1}$ .

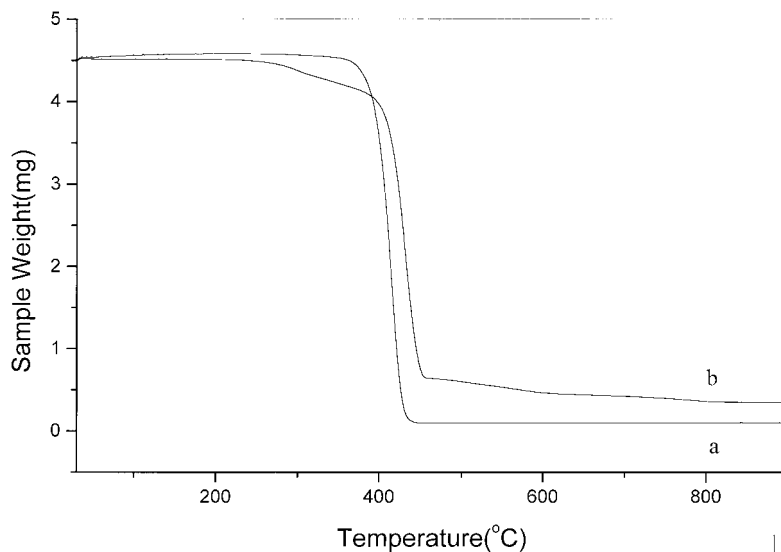


**Figure 4** TGA curves of (a) pristine polystyrene and (b) as-prepared nanocomposite material. The heating rate was  $10^{\circ}\text{C min}^{-1}$ .

of the nickel nanoparticles in the polystyrene matrix at 1.6 Tesla did not reach full saturation and shows a very weak hysteresis. This deviation is undoubtedly a result of the nanostructure of the sample. The magnetization of a specimen consisting of small particles decreases with a decreasing particle size due to the increased dispersion in the exchange integral,<sup>34</sup> finally reaching a superparamagnetic state in which each particle acts as a big spin with a suppressed exchange interaction between the particles. For a theoretical description of the magnetic behavior of interacting nanoparticles, see ref. 34.

#### Mechanism for the formation of nickel-polystyrene nanocomposite

Ultrasonic waves, which are intense enough to produce cavitation, can drive chemical reactions such as

oxidation, reduction, dissolution, decomposition, and hydrolysis.<sup>23,35-37</sup> Other reactions, such as the promotion of polymerization, have also been reported to be induced by ultrasound. There are two regions of sonochemical activity, as postulated by Suslick and co-workers<sup>38,39</sup>: inside the collapsing bubble and at the interface between the bubble and the liquid. If the reaction takes place inside the collapsing bubble, as is the case for transition-metal carbonyls dissolved in organic solvents, the temperature inside the cavitation bubble can be 5000 K depending on the vapor pressure of the solvent.<sup>38</sup> If water is used as the solvent, the maximum bubble core temperature that can be reached is close to 4000 K,<sup>35</sup> causing the pyrolysis of water to H and OH radicals. The sonolysis of DMF produces  $\text{CH}_3$  and  $\text{N}(\text{CH}_3)\text{CHO}$  radicals.<sup>40</sup> The mechanism of the formation of nickel nanoparticles in poly-

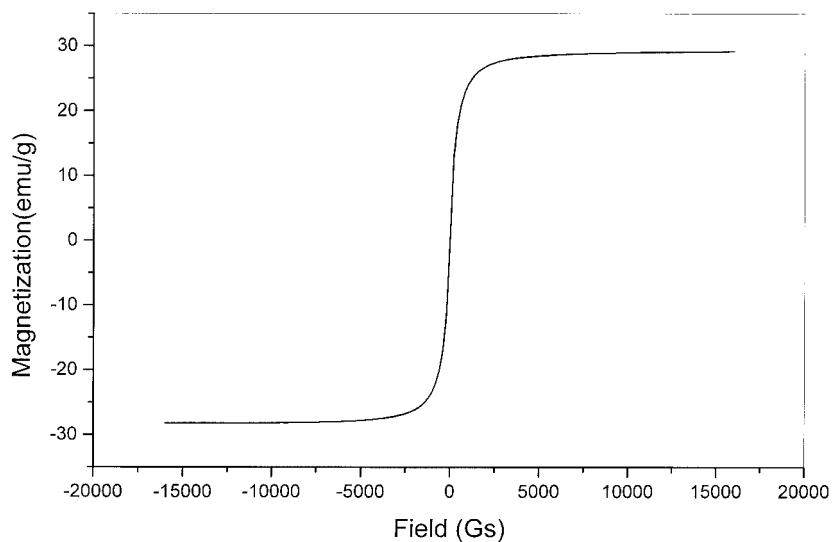
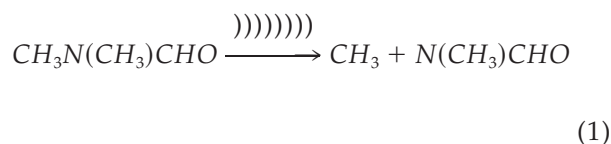
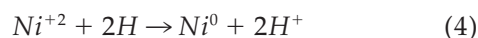
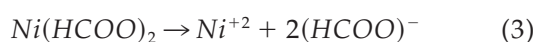
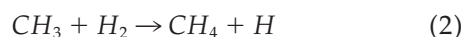


**Figure 5** Room-temperature magnetization loop of as-prepared nanocomposite material.

styrene takes into consideration the radical species generated from the DMF molecule by ultrasound irradiation:



In an argon and hydrogen atmosphere, H radicals are produced from hydrogen abstraction by the methyl radicals<sup>41</sup>:



A decrease in the pH from 8.3 to 7.1 after the reaction indicates the generation of H<sup>+</sup> ions during sonication. The sonochemical reduction process generates high temperatures and pressures for the reduction of nickel formate to metallic nickel. A controlled experiment was carried out in which nickel formate and polystyrene in DMF were sonicated for 3 h under argon. No precipitate of Ni was observed. The reduction of nickel formate in polystyrene under the same reaction conditions (Ar/H<sub>2</sub>), however, with fast stirring instead of sonication, did not lead to the formation of nickel nanoparticles in the polystyrene. It is known that nickel formate yields nickel powder by heating the nickel formate in the presence of air at 250–300°C.<sup>29</sup> This confirms that the transient high temperatures and fast cooling rates, generated under sonochemical conditions, are necessary for reduction to occur.

## CONCLUSIONS

Uniformly dispersed nickel nanoparticles in polystyrene were prepared by ultrasound irradiation. The magnetic properties of this nanocomposite material established that the nanocomposite material is superparamagnetic in nature. The starting material is non-toxic safe and avoids the use of nickel carbonyl. This method can also be used to prepare other metal-polymer nanocomposite materials from corresponding metal formates and polymers.

One of the authors (R. V. K.) thanks the Bar-Ilan Research Authority for his postdoctoral fellowship. One of the authors (A. G.) thanks the Israeli Ministry of Science, Culture and Sports for supporting this research via an Infrastructure grant and also thanks the German Ministry of Science through the Deutsche-Israel program, DIP, for its support.

This project was also partially supported by an INTAS grant. The authors are grateful to Prof. Z. Malik, Department of Life Sciences, for extending their facilities to them. The authors also thank Prof. Y. Yeshurun for making available the facilities of the National Center for Magnetic Measurements at the Department of Physics, Bar-Ilan University, for this study.

## References

1. Antonietti, M.; Giltner, C. *Angew Chem Int Ed Engl* 1997, 36, 910.
2. Schmid, G. *Clusters and Colloids*; VCH: Weinheim, 1994.
3. Fendler, J. H. *Nanoparticles and Nanostructured Films*; Wiley-VCH: Weinheim, 1998.
4. Henglein, A. *Chem Rev* 1989, 89, 1861.
5. Bigg, D. M. *Polym Compos* 1986, 7, 125.
6. Schmid, G. *Chem Rev* 1992, 92, 1709.
7. Hirai, H.; Wakabayashi, H.; Komiyama, M. *Bull Chem Soc Jpn* 1986, 59, 367.
8. Noguchi, T.; Gotoh, K.; Yamaguchi, Y.; Deki, S. *J Mater Sci Lett* 1991, 10, 477.
9. Deki, S.; Akemsatsu, K.; Yano, T.; Mizuhata, M.; Kajinami, A. *J Mater Chem* 1998, 8, 1865.
10. Spatz, J. P.; Mossmer, S.; Moller, M. *Angew Chem Int Ed* 1996, 35, 1510.
11. Spatz, J. P.; Roescher, A.; Moller, M. *Adv Mater* 1996, 8, 337.
12. Spatz, J. P.; Mossmer, S.; Moller, M. *Chem Eur J* 1996, 2, 1552.
13. Antonietti, M.; Thonemann, A.; Wenz, E. *Colloid Polym Sci* 1996, 274, 795.
14. Zhou, Y.; Hao, L. Y.; Yu, S. H.; You, M.; Zhu, Y. R.; Chen, Z. Y. *Chem Mater* 1999, 11, 3411.
15. Huang, C.; Yang, C. Z. *Appl Phys Lett* 1999, 74, 1692.
16. Lyons, A. M.; Nakahara, S.; Marcus, M. A.; Pearce, E. M.; Waszczak, J. V. *J Phys Chem* 1991, 95, 1098.
17. Sidorov, S. N.; Bronstein, L. M.; Davankov, V. A.; Tsyurupa, M. P.; Solodovnikov, S. P.; Valestky, P. M.; Wilder, E. A.; Sponatak, R. J. *Chem Mater* 1999, 11, 3210.
18. Zach, M. P.; Penner, R. M. *Adv Mater* 2000, 12, 878.
19. Chen, D. H.; Wu, S. H. *Chem Mater* 2000, 12, 1354.
20. Ely, T. O.; Amiens, C.; Chaudret, B.; Snoeck, E.; Verelst, M.; Respaud, M. M.; Broto, J. M. *Chem Mater* 1999, 11, 526.
21. Wang, P. H.; Pan, C. Y. *Colloid Polym Sci* 2000, 278, 581.
22. *Ultrasound: Its Chemical Physical and Biological Effects*; Suslick, K. S., Ed.; VCH: Weinheim, 1988.
23. Suslick, K. S.; Choe, S. B.; Cichowals, A. A.; Grinstaff, M. W. *Nature* 1991, 353, 414.
24. Koltypin, Y.; Katabi, G.; Cao, X.; Prozorov, R.; Gedanken, A. *J Non-Cryst Solids* 1996, 201, 159.
25. Zhong, Z.; Mastai, Y.; Koltypin, Y.; Zhao, Y. M.; Gedanken, A. *Chem Mater* 1999, 11, 2350.
26. Ramesh, S.; Koltypin, Y.; Prozorov, R.; Gedanken, A. *Chem Mater* 1997, 9, 546.
27. Koltypin, Y.; Fernandez, A.; Rojas, T. C.; Campora, J.; Palma, P.; Prozorov, R.; Gedanken, A. *Chem Mater* 1999, 11, 1331.
28. (a) Wizel, S.; Prozorov, R.; Cohen, Y.; Aurbach, D.; Margel, S.; Gedaken, A. *J Mater Res* 1998, 13, 211; (b) Wizel, S.; Margel, S.; Roja, T. C.; Fernandez, A.; Prozorov, R.; Gedanken, A. *J Mater Res* 1999, 14, 3913; (c) Wizel, S.; Margel, S.; Gedanken, A. *Polym Int* 2000, 49, 445; (d) Vijaya Kumar, R.; Koltypin, Y.; Cohen, Y. S.; Cohen, Y.; Aurbach, D.; Palchik, O.; Felner, I.; Gedanken, A. *J Mater Chem* 2000, 10, 1125.
29. Francisco, J. F. *J Chem Ed A* 1995, 72, 201.

30. Klug, H.; Alexander, L. *X-ray Diffraction Procedures*; Wiley: New York, 1962; p 125.
31. Penczek, P.; Rudnik, E.; Arcyzewska, B.; Ostrysz, R. *Angew Makromol Chem* 1995, 229, 15.
32. Levchik, G. F.; Si, K.; Levchik, S. V.; Camino, G.; Wilkie, C. A. *Polym Degrad Stab* 1999, 65, 395.
33. Hwang, J. H.; Dravid, V. P.; Teng, M. H.; Host, J. J.; Elliott, B. R.; Johnson, D. L.; Mason, T. O. *J Mater Res* 1997, 12, 1076.
34. Elliott, S. R. *Physics of Amorphous Materials*; Longman: London, New York, 1984; p 350.
35. Gutierrez, M.; Henglein, A. *J Phys Chem* 1988, 92, 2978.
36. Sostaric, J. Z.; Mulvaney, P.; Grieser, F. *J Chem Soc Faraday Trans* 1995, 91, 2843.
37. Gutierrez, M.; Henglein, A.; Dohrmann, J. *J Phys Chem* 1987, 91, 6687.
38. Mc Namara, W. B., III; Didenko, Y. T.; Suslick, K. S. *Nature* 1999, 401, 772.
39. (a) Suslick, K. S.; Hammerton, D. A.; Chine, R. E. *J Am Chem Soc* 1986, 108, 5641; (b) Grinstaff, M. W.; Cichowlass, A. A.; Choe, S. B.; Suslick, K. S. *Ultrasonics* 1992, 30, 168.
40. Vladimir, M.; Riesz, P. *J Phys Chem* 1994, 98, 1634.
41. Vladimir, M.; Kirschenbaum, L. J.; Riesz, P. *J Phys Chem* 1995, 99, 5970.